

Electrostatically Induced Polyelectrolyte Association of Rodlike Virus Particles

Alexander P. Lyubartsev,^{1,*} Jay X. Tang,² Paul A. Janmey,² and Lars Nordenskiöld¹

¹*Physical Chemistry, Arrhenius Laboratory, Stockholm University, S-10691 Stockholm, Sweden*

²*Hematology Division, Brigham and Women's Hospital, Harvard Medical School,*

LMRC 301, 221 Longwood Avenue, Boston, Massachusetts 02115

(Received 27 April 1998)

Calculations of the electrostatic osmotic pressure for a closely packed phase of laterally ordered rodlike fd or M13 virus particles at equilibrium with a bulk salt solution have been performed using grand canonical Monte Carlo simulations. With increasing concentration of divalent counterions, the pressure becomes attractive. The attraction is stronger for higher surface charge density (of fd virus as opposed to M13 virus) and smaller counterion radius. The calculations agree with the results from light scattering measurements, which sensitively detect the formation of laterally ordered virus aggregates. [S0031-9007(98)07969-1]

PACS numbers: 87.15.Da

Many cylindrical (rodlike) biopolymers such as DNA and F-actin are highly negatively charged polyelectrolytes that frequently occur in compact and ordered forms *in vivo* [1]. Recently, much attention has been focused on theoretical treatments of the phenomenon of electrostatic attraction between like-charged cylindrical polyelectrolytes in aqueous medium, which is induced by multivalent counterions [2–4]. This effect is not predicted by the standard treatment of electrostatics in polyelectrolyte systems, based on the mean field Poisson-Boltzmann equation [5], which always predicts a repulsive force between similarly charged surfaces. Salt-induced condensation of polyelectrolytes is frequently observed experimentally, and the mechanism of the attraction has been proposed to be the instantaneously correlated fluctuations in the interaction between the ion clouds associated with the polyelectrolytes. The presence of this effect is reminiscent of the quantum mechanical attractive London dispersion force and has been known for quite some time [5,6].

The interest in this problem for cylindrical polyelectrolytes is largely related to the formation of condensed forms of DNA upon addition of multivalent counterions to an isotropic DNA solution [7]. Recently, other negatively charged rodlike biopolyelectrolyte systems such as F-actin and the bacteriophage fd have also been shown to form laterally ordered aggregates (henceforth called bundles) due to the presence of multivalent counterions [8]. This fact strongly suggests that attractive electrostatic interactions are both feasible and relevant for biological polyelectrolytes. It is therefore of considerable importance to obtain relevant experimental data for different systems under varying conditions and make accurate comparison with theoretical predictions of electrostatic forces, performed under the same conditions as the experiments.

Two strains of *Inovirus*, the bacteriophages with generic designations fd and M13, are suitable model biopolyelectrolytes to study bundle formation. They are long and stiff rodlike particles. Each virus is coated by approximately 2700 copies of identical polypeptides that cover the inte-

rior single stranded, closed DNA [9], giving the virions a length of 880 nm and a diameter of 6.5 nm. M13 and fd differ by a single amino acid in their major coat protein subunit, a 50-amino-acid α -helical polypeptide. As a result of this difference, M13 has one negative charge less per subunit than fd, corresponding to approximately a 30% reduction in surface charge density. In this Letter, we present light scattering experiments that define the conditions required for bundle formation by Ca^{2+} and Mg^{2+} of fd and M13 viruses. Grand canonical Monte Carlo simulations have been used to calculate the osmotic pressure versus inter-rod separation for ordered arrays of charged rods in equilibrium with a bulk salt solution corresponding to the experimental conditions. This is the first time that a combined experimental and quantitative simulation study of polyelectrolyte bundling has been performed. This direct application of simulation to a specific experimental system is made possible by performing the Monte Carlo simulations within the grand canonical ensemble, which enables variation of the bulk salt content corresponding to the experimental situation.

Light scattering measurements and preparation of the fd and M13 phages were performed as described previously [8]. The virus suspensions were kept in a low ionic strength buffer containing 2 mM HEPES, pH 7.0, and 1 mM NaN_3 . 600 μl of 0.1 mg/ml virus was used for each measurement. The initial scattering intensities for the solutions of both fd and M13 viruses were the same within experimental variation. Each subsequent reading in the figures represents a scattering intensity measured when the solution reached a steady state following addition of stock solution of CaCl_2 or MgCl_2 .

Monte Carlo simulations were performed for a model system consisting of an infinite array of hexagonally packed polyelectrolyte rods separated by a variable distance r (distance between the polyion surfaces), with mobile ions between them. The fd and M13 virions and the electrostatic interactions have been modeled as depicted in Fig. 1 [10]: The rods are described as infinitely long

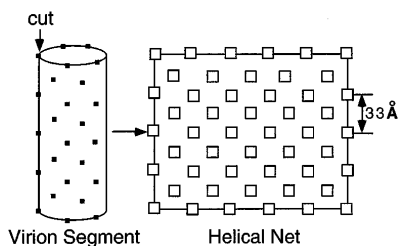


FIG. 1. Schematics of positioning of the charges on the viral surface. Left: Positions of protein subunits on a segment of fd or M13 virus. Right: Helical net of the viral surface, viewed by cutting and unfolding the cylindrical surface. One negative charge is placed at every corner of the small squares as shown for fd.

hard cylinders of diameter $a = 6.0$ nm and with discrete negative charges at the surface of the rod. The positions of the four (fd) or three (M13) negative charges form a square (fd) or unilateral triangle (M13) of 10 \AA on each side, representing a protein subunit, whose centers are placed at the surface of the cylinder as obtained from the crystallographic packing of the subunits [9] (Fig. 1). This arrangement gives average axial linear charge separations $b = 0.825$ and 1.1 \AA , for fd and M13, respectively. The solvent water is treated as a dielectric continuum described by a dielectric permittivity $\epsilon = 78$ at a temperature $T = 300$ K. The mobile ions and the rod charges are described as point charges $q_i = z_i e$, with a repulsive r^{-12} potential of effective hydrated diameter d_i . The value of d_i is set to 4 \AA for the monovalent mobile ions with $z_i = \pm 1$, as well as for the negative charges on the rod, thus making the effective rod diameter 6.4 nm. The diameter d_i for the divalent ions can be varied and this is then a way to take into account not just the bare diameter of the counterions, but also the effects of the solvent water on the effective hydration of the multivalent ions in an averaged form. The total potential energy of the system (excluding the hard rod term) is

$$U = \sum_{i,j} \frac{q_i q_j}{4\pi\epsilon_0\epsilon r_{ij}} + kT \sum_{i,j} \left(\frac{d_i + d_j}{2r_{ij}} \right)^{12}, \quad (1)$$

where $r_{ij} = |r_i - r_j|$ is the distance between ions i and j .

The calculations have been performed in a simulation "box" in the form of a hexagonal prism containing one rod of height $h = 9.9$ nm and length L , defined by the given variable rod-rod separation r : $L = (r + a)/\sqrt{3}$. Periodic boundary conditions were applied in all directions, and the long-range electrostatic interactions from the lattice of surrounding cells were included as in a previous work [2] by the Ewald summation method.

In the experiments, the well-defined salt concentration of the bulk is in equilibrium with the ordered phase, whose salt content is determined by the condition of equilibrium between the phases. Therefore, the Monte Carlo simulations have been performed within the grand canonical ensemble under the condition of equal chemical potential in the phases [8], obtained from separate simulations

of the bulk electrolyte solution. The relative osmotic pressure, p_{osm} , is

$$p_{\text{osm}} = p_{\text{rod}}(r) - p_{\text{bulk}}. \quad (2)$$

Here $p_{\text{rod}}(r)$ is the pressure of the ordered rod phase at separation r and p_{bulk} is the pressure of the bulk phase. Within the grand canonical ensemble the pressure in either of the two systems is thus given by

$$p = kT \left. \frac{\partial \ln(\Xi)}{\partial V} \right|_{T,\mu}. \quad (3)$$

Here Ξ is the grand canonical partition function and μ the chemical potential of the system. The right hand side of Eq. (3) has been evaluated for varying distances r , using the expanded ensemble method [2,11].

In the simulations, the bulk has been modeled as a mixture of 2:1 and 1:1 salt, MeX_2/MX , where $z_{\text{Me}} = +2$, $z_X = -1$, and $z_M = +1$. The concentration of divalent salt has been varied while the monovalent salt is kept constant at 2 mM, in accordance with the experiments. Here Me stands for a divalent metal ion (Mg or Ca), X for a monovalent ion (Cl), and M for a monovalent metal ion (Na).

Figure 2 shows the osmotic pressure curves, obtained from the Monte Carlo simulations for fd [Fig. 2(a)] and

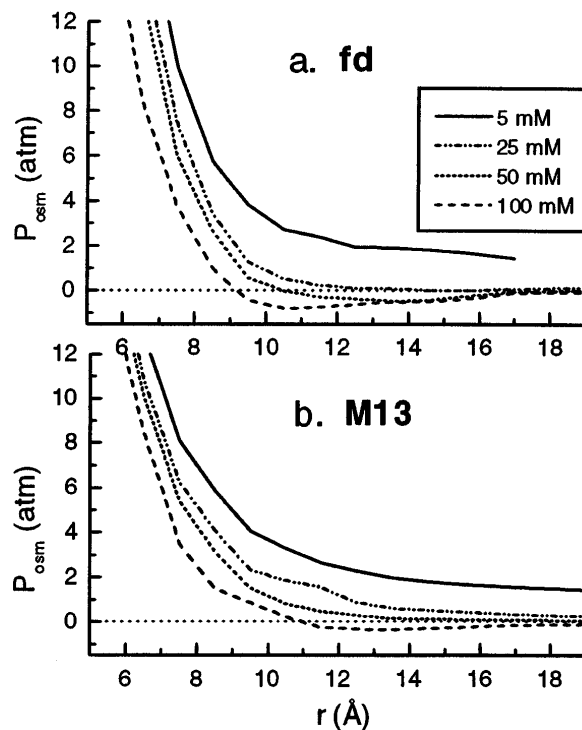


FIG. 2. The calculated osmotic pressure p_{osm} (in atm), as a function of rod-rod surface separation r , for the ordered fd (a) and M13 (b) virus systems, respectively. The different curves have been calculated for varying divalent salt concentrations as indicated in the inset. All calculations are for divalent counterion diameter $d_{\text{Me}} = 5 \text{ \AA}$.

M13 [Fig. 2(b)], respectively, for varying amounts of total divalent salt concentrations in the bulk. The calculations are for a divalent ion diameter $d_{Me} = 5 \text{ \AA}$. For the fd virus system with higher surface charge density [Fig. 2(a)] the general feature of the pressure curve is a repulsive interaction at all rod-rod separations for low concentrations of added divalent salt. At increasing divalent counterion concentrations, the pressure becomes less repulsive at intermediate distances (around 10 \AA). Further increase of the divalent salt leads to an attractive minimum positioned at about 11 \AA . For this system the attractive force appears when the concentration $[MeX_2]$ in the bulk is larger than 25 mM but less than 50 mM . The results for the M13 system show the same general trend as the fd virus but with the important difference that a larger amount of divalent salt must be added to this less charged polyelectrolyte in order to obtain an attractive pressure curve. For M13 the onset of attraction starts at a concentration of about 70 mM divalent salt.

A critical parameter for our simulations is the value of the hydrated ion diameter d_{Me} . Figure 3 shows simulation results obtained with a larger divalent ion diameter $d_{Me} = 6 \text{ \AA}$. The general form of the pressure curves for the two systems is similar to that seen in Fig. 2, but there are significant quantitative differences. Comparing the results for fd in Figs. 2(a) and 3(a) shows that the onset of attraction is displaced from about 25 to about 50 mM when increasing the divalent ion diameter from 5 to 6 \AA . A similar effect is observed [Figs. 2(b) and 3(b)] for M13.

The static light scattering experiment provides an accurate method to detect bundling, due to the steep increase

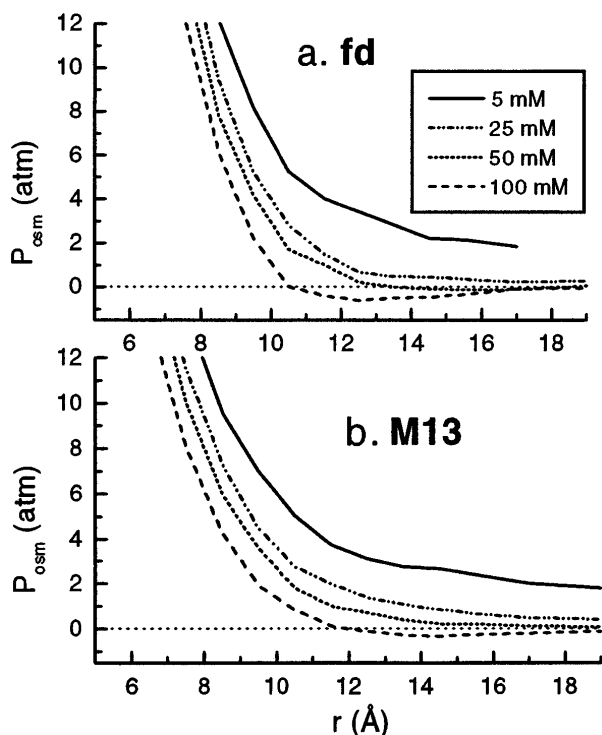


FIG. 3. As in Fig. 2 but for $d_{Me} = 6 \text{ \AA}$.

in scattering upon formation of laterally ordered aggregates [8]. Figure 4 shows the bundling of behavior for fd and M13 due to addition of the divalent salt CaCl_2 or MgCl_2 . A higher concentration of CaCl_2 is needed to induce bundling of M13 (about 60 mM CaCl_2) compared to fd (about 45 mM CaCl_2). For fd, a greater magnesium ion concentration (about 75 mM) is needed to induce bundling as compared to the calcium counterion (about 45 mM). For M13 MgCl_2 does not form bundles at any experimentally achievable concentration up to 1 M .

Comparison of the experimental measurements of fd and M13 virus bundling with the calculated osmotic pressure curves is presently at a qualitative level, since a truly quantitative prediction of bundling from theory requires calculation of the free energy difference between bundled and dissolved states and would assume that no other interactions are significant. The general behavior of the pressure curves in Figs. 2 and 3 is that addition of divalent salt leads to the appearance of a net attraction, consistent with the bundling induced by increasing amounts of Ca^{2+} in the case of fd and M13, and by Mg^{2+} for fd. Furthermore, the experimental observation that more Ca^{2+} is needed for bundling of the less charged M13 is also qualitatively confirmed by the calculated pressure curves. In addition, the concentrations of divalent counterions as well as the difference in amounts needed for the appearance of attraction in the fd and M13 systems in Fig. 2 correspond reasonably closely to the experimental values for bundling by Ca^{2+} seen in Fig. 4.

The experimental differences observed between Ca^{2+} and Mg^{2+} can be rationalized by the difference in hydrated size of these ions in aqueous solution [12,13]. The Mg^{2+} ion with a smaller naked ion radius has a larger effective hydrated ion radius than the Ca^{2+} ion. It should be noted in this context that the two different hydrated diameters used in the simulations, 5 and 6 \AA , are merely approximate and reasonable choices of this parameter [13]. This dependence of the attraction on ion radius has been noted in previous calculations [2,3].

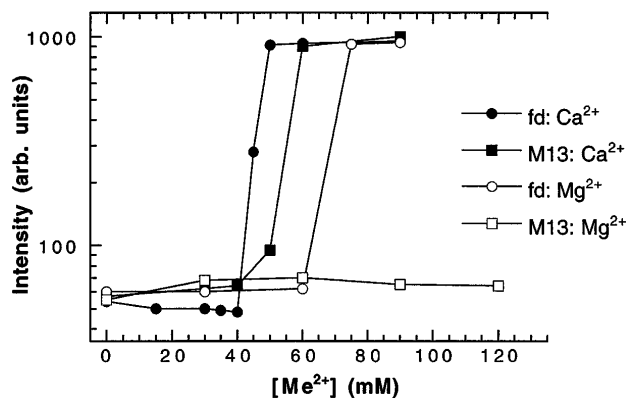


FIG. 4. Light scattering intensities for fd and M13 virus solutions as a function of Ca^{2+} and Mg^{2+} concentrations (as indicated in the legend), following sequential additions of CaCl_2 and MgCl_2 .

An important issue of broad interest is the question whether the equilibrium state of the system is one infinite bundle or several large but finite bundles [14]. We have made an additional simulation for three fd-like rods in a hexagonal cell, removing the periodic boundary condition in the XY directions, thus modeling a finite bundle of three polyions (calculations were made for $d_{Me} = 5 \text{ \AA}$, $[MeX_2] = 100 \text{ mM}$, and $r = 10.5 \text{ \AA}$). The osmotic pressure was $-0.4 \pm 0.1 \text{ atm}$, whereas for the corresponding infinite system it was $-1.1 \pm 0.1 \text{ atm}$. Within the calculation error this corresponds to the difference in the number of neighbors in the finite and infinite systems (2 and 6, respectively) and the effective interaction between the polyions thus appears to be essentially pairwise additive between nearest neighbors. This is due to the fact that the interaction between the polyions is of short range (compared to the diameter), and therefore interactions with polyions outside the nearest neighbors are of minor importance [15]. Larger bundles should then be more stable mainly due to more pairwise interactions, an effect that is expected to become less important with increasing size. In the experiments we observe a slow kinetics of bundling at the onset bundling condition [8]. A stable scattering intensity may require over an hour to occur, but eventually bundles of hundreds or even thousands of virus filaments were detected [8]. The slow process may be attributed to the low initial driving force for pair formation in small bundles. It is also worth noting that due to many higher order effects such as loss of orientational entropy accompanied by the growth of large bundles, bundles with finite final size are expected and indeed experimentally observed.

In conclusion, the present study has shown that the grand canonical expanded ensemble Monte Carlo simulations give excellent qualitative prediction of the experimentally determined bundling behavior of fd and M13 viruses. The general agreement between the Monte Carlo predictions and the experimental data provides clear evidence that the bundling behavior is largely determined by electrostatic attraction induced by the presence of multivalent counterions. It must, however, be stressed that the model contains several important simplifications. The dielectric continuum model is clearly a serious approximation, although the presence of an effective hydrated ion radius, to some extent, is a way of including effects due to the molecular nature of the aqueous solvent, as well as the specificity of different ions. Furthermore, the molecu-

lar detail of the polyelectrolyte virus systems is basically neglected.

This work has been supported by the Swedish Natural Science Research Council, NFR (L.N.), the Swedish Royal Academy of Sciences, KVA (A.L. and L.N.), and by a National Institute of Health (NIH) grant (AR38910) (P.J.).

*On leave from The Scientific Research Institute of Physics, St. Petersburg State University, 198904 St. Petersburg, Russia.

Email address: lnor@phycs.su.se

- [1] J. Darnell, H. Lodish, and D. Baltimore, *Molecular Cell Biology* (Scientific American Books, New York, 1986).
- [2] A. P. Lyubartsev and L. Nordenskiöld, *J. Phys. Chem.* **99**, 10373 (1995).
- [3] N. Grønbech-Jensen, R.J. Mashl, R.F. Bruinsma, and W.M. Gelbart, *Phys. Rev. Lett.* **78**, 2477 (1997).
- [4] B.-Y. Ha and A.J. Liu, *Phys. Rev. Lett.* **79**, 1289 (1997).
- [5] L. Guldbrand, L. Nilsson, and L. Nordenskiöld, *J. Chem. Phys.* **85**, 6686 (1986).
- [6] F. Oosawa, *Biopolymers* **6**, 1633 (1968).
- [7] V. A. Bloomfield, *Curr. Opin. Struct. Biol.* **6**, 334 (1996).
- [8] J. X. Tang, S. Wong, P. T. Tran, and P. A. Janmey, *Ber. Bunsen-Ges. Phys. Chem.* **100**, 796 (1996).
- [9] L. A. Day, C. J. Marzec, S. A. Reisberg, and A. Casadevall, *Annu. Rev. Biophys. Biophys. Chem.* **17**, 509 (1988).
- [10] S. Battacharjee, M. J. Glucksman, and L. Makowski, *Biophys. J.* **61**, 725 (1992).
- [11] A. P. Lyubartsev, A. A. Martsinovskii, S. V. Shevkunov, and P. N. Vorontsov-Velyaminov, *J. Chem. Phys.* **96**, 1776 (1992).
- [12] M. D. Paulsen, C. F. Anderson, and M. T. Record, Jr., *Biopolymers* **27**, 1249 (1988).
- [13] H. R. Corti and R. Fernandez-Prini, *J. Chem. Soc. Faraday Trans. 2* **82**, 921 (1986).
- [14] This issue will be further discussed in a future work presenting additional simulations and experimental results.
- [15] It should be noted that the fact that a nearest neighbor approximation seems to be valid does not relate to the question of pairwise additivity in the interparticle interaction. Furthermore, the question of the relation between the number of polyions to the magnitude of the correlated fluctuations is outside the scope of the present Letter and will be discussed elsewhere. See also (a) R. Podgornik and V. A. Parsegian, *Phys. Rev. Lett.* **80**, 1560 (1998); (b) B.-Y. Ha and A. J. Liu, *Phys. Rev. Lett.* **81**, 1011 (1998).